

JLab PAC12 Proposal Cover Sheet

This document must be received by ~~closed~~ business day before 1997

Jefferson Lab
User Liaison Office, Mail Stop 12 B
12000 Jefferson Avenue
Newport News, VA 23606

(Choose one)

- New Proposal Title:
 Update Experiment Number: **E-94-020**
 Letter-of-Intent Title:

Contact Person

Name: **W. Korsch (University of Kentucky), R. McKeown (Caltech),**
Institution: **University of Kentucky** **Z.-E. Meizani (Temple)**
Address: **177 Chemistry-Physics Bldg.**
Address:
City, State, ZIP/Country: **Lexington, KY 40506**
Phone: **606-257-4083** Fax:
E-Mail: **KORSCH@PA.UKY.EDU, BMCKEKRL.CALTECH.EDU, MEZIANI@VM.TEMPLE.EDU**

Experimental Hall: **R**

Days Requested for Approval: **15**

Jefferson Lab Use Only

Receipt Date: **6/26/97**

By: _____

PR 97-013

LAB RESOURCES LIST

JLab Proposal No.: E-94-020
(For JLab ULO use only.)

Date 6/25/97

List below significant resources — both equipment and human — that you are requesting from Jefferson Lab in support of mounting and executing the proposed experiment. Do not include items that will be routinely supplied to all running experiments such as the base equipment for the hall and technical support for routine operation, installation, and maintenance.

Major Installations (either your equip. or new equip. requested from JLab)

Polarized ^3He Target

New Support Structures: _____

Data Acquisition/Reduction

Computing Resources: _____

New Software: _____

Major Equipment

Magnets: _____

Power Supplies: _____

Targets: _____

Detectors: _____

Electronics: _____

Computer Hardware: _____

Other: _____

Other: _____

HAZARD IDENTIFICATION CHECKLIST

Lab Proposal No.: E-94-020
(For CEBAF User Liaison Office use only.)

Date: _____

Check all items for which there is an anticipated need.

<p>Cryogenics</p> <p>_____ beamline magnets _____ analysis magnets _____ target type: _____ flow rate: _____ capacity: _____</p>	<p>Electrical Equipment</p> <p>_____ cryo/electrical devices _____ capacitor banks _____ high voltage _____ exposed equipment</p>	<p>Radioactive/Hazardous Materials List any radioactive or hazardous/toxic materials planned for use:</p> <p>_____ _____ _____ _____</p>
<p>Pressure Vessels</p> <p>_____ inside diameter _____ operating pressure _____ window material _____ window thickness</p>	<p>Flammable Gas or Liquids</p> <p>type: _____ flow rate: _____ capacity: _____</p> <p>Drift Chambers</p> <p>type: _____ flow rate: _____ capacity: _____</p>	<p>Other Target Materials</p> <p>___ Beryllium (Be) ___ Lithium (Li) ___ Mercury (Hg) ___ Lead (Pb) ___ Tungsten (W) ___ Uranium (U) <input checked="" type="checkbox"/> Other (list below) <u>3He, N₂, Rb</u></p>
<p>Vacuum Vessels</p> <p>_____ inside diameter _____ operating pressure _____ window material _____ window thickness</p>	<p>Radioactive Sources</p> <p>_____ permanent installation _____ temporary use</p> <p>type: _____ strength: _____</p>	<p>Large Mech. Structure/System</p> <p>_____ lifting devices _____ motion controllers _____ scaffolding or _____ elevated platforms</p>
<p>Lasers</p> <p>type: <u>Laser Diode System</u> wattage: <u>100 W</u> class: <u>IV</u></p> <p>Installation: _____ <input checked="" type="checkbox"/> permanent* _____ temporary</p> <p>* <u>For experiment</u> Use: _____ calibration _____ alignment</p> <p><u>For 3He target</u></p>	<p>Hazardous Materials</p> <p>_____ cyanide plating materials _____ scintillation oil (from) _____ PCBs _____ methane _____ TMAE _____ TEA _____ photographic developers _____ other (list below)</p> <p>_____ _____</p>	<p>General:</p> <p>Experiment Class:</p> <p>_____ Base Equipment _____ Temp. Mod. to Base Equip. _____ Permanent Mod. to Base Equipment _____ Major New Apparatus</p> <p>Other: _____ _____</p>

Investigation of the ^3He wave function using the $^3\vec{\text{He}}(\vec{e}, e'p)d$ and the $^3\vec{\text{He}}(\vec{e}, e'p)pn$ Reactions

W.J. Cummings, H. Gao, O. Hansen

Argonne National Laboratory, Argonne, IL 60439

T. Averett, B. Filippone, C. Jones, R. McKeown (co-spokesperson)

California Institute of Technology, Pasadena, CA 91101

J.P. Chen, K. de Jager, J. Gomez, J. LeRose, M. Liang, R. Michaels,
S. Nanda, A. Saha, B. Wojtsekowski

TJNAF, Newport News, VA 23606

B. Anderson, R. Madey, D.M. Manley, G.G. Petratos, J. Watson

Kent State University, Kent, OH 44242

D. Dale, T. Gorringer, W. Korsch (co-spokesperson), M. Kovash, V. Zeps

University of Kentucky, Lexington, KY 40506

P. Bogorad, G.D. Cates, K. Kumar

Princeton University, Princeton, NJ 08544

C. Glashauser, R. Gilman, R.D. Ransome, P. Rutt

Rutgers University, Rutgers, NJ 08855

R. Holmes, J. McCracken, P.A. Souder, X. Wang

Syracuse University, Syracuse, NY 13210

L. Auerbach, Z. Dziembowski, J. Martoff, Z.-E. Meziani (co-spokesperson), J. Park

Temple University, Philadelphia, PA 19122

M. Pitt

Virginia Polytechnic Institute, Blacksburg, VA 24061

I. Physics Motivation

The study of few body systems, especially the ${}^3\text{He}$ nucleus, has been of great interest in the last years, since both experimental and theoretical techniques have improved to a level that high precision studies on the 3 body system can be performed. Many experiments all over the world are devoted to study fundamental properties of the neutron, using ${}^3\text{He}$ as an effective neutron target. With new developments in laser technology one is able to produce highly polarized ${}^3\text{He}$ targets in the form of internal targets which are intalled inside a storage ring [1, 2] or external targets with densities of up to 10^{22} atoms/cm² [3, 4, 5, 6]. There are also already three approved experiments at Jefferson Lab [7] which use a polarized ${}^3\text{He}$ target to measure the electromagnetic formfactors and the spin structure of the neutron. Since these experiments aim for high precision, it is very important to understand how nuclear structure effects can influence the extraction of neutron properties. Theoretically, one can now solve the three body system exactly by means of solving the corresponding Faddeev equations [9]. However, due to the different treatment of the nucleon-nucleon isospin dependence and tensor forces most existing calculations show some scatter in their predictions for the triton binding energy. Nearly all calculations underestimate the triton binding energy by about 0.9 MeV (the experimental value is 8.48 MeV). The effect of three-nucleon forces is hardly addressed at all. Since the ${}^3\text{He}$ nucleus consists of two protons and one neutron, where the probability of finding the neutron in a spatial S-part of the wave-function is about 0.87, the nuclear spin of ${}^3\text{He}$ is more or less completely carried by the neutron (both proton spins add up to zero). This means a polarized ${}^3\text{He}$ nucleus can be envisaged to a good approximation as a polarized neutron. However, due to the isospin dependence and tensor force in the nucleon-nucleon interaction, the neutron can also be found in part in the spatially mixed S' -state, at low missing momenta, and in the D-state, at higher missing momenta. The S' state has both proton spins paired parallel to the spin of the nucleus whereas in the D-state the spins of the nucleons are antiparallel to the orbital momentum $L=2$ and therefore antiparallel to the ${}^3\text{He}$ spin. Friar *et al.* [10] give an estimate for the S' -state probability of 2.8%. The D-wave contribution is of the order 10%. The CE25 experiment demonstrated at IUCF the power of a polarized ${}^3\text{He}$ target, by extracting a *proton* polarization of $-12\pm 2\%$ from the ${}^3\vec{\text{He}}(\vec{p}, 2p)$ reaction at low missing momentum [11]. This number is consistent with S and S' states as calculated in Faddeev calculations.

Therefore, we propose to perform a precision measurement using the ${}^3\vec{\text{He}}(\vec{e}, e'p)d$ and ${}^3\vec{\text{He}}(\vec{e}, e'p)pn$ reactions which will allow us to study the effects of the S' - and D-states at a Q^2 of 1.0 GeV/c². We plan to perform this experiment in Hall A using both high resolution spectrometers (HRS).

II. Discussion of the Experiment

We plan to investigate the ${}^3\text{He}$ wave-function using the ${}^3\text{He}(\bar{e}, e'p)d$ reaction as function of missing momentum p_m at a Q^2 of $1.0 \text{ GeV}^2/c^2$. The proposed measurements are motivated by the results of a calculation by Laget [12].

In the case of polarized beam and polarized target, the $(e, e'N)$ cross-section can be written in the following way (we follow here the notation of Laget [13]):

$$\frac{d\sigma(h, \vec{S})}{d\Omega_e dE_e d\Omega_p dp_p} = \frac{d\sigma^0}{d\Omega_e dE_e d\Omega_p dp_p} \cdot [1 + \vec{S} \cdot \vec{A}^0 + h(A_e + \vec{S} \cdot \vec{A}')] , \quad (1)$$

where h is the helicity of the electron ($+1/-1$), \vec{S} is the spin of the target, σ^0 is the unpolarized cross-section, \vec{A}^0 is the target analyzing power, or target asymmetry, \vec{A}' is the spin correlation parameter, or spin transfer asymmetry. The quantization axis is chosen to be along the direction of the momentum of the virtual photon. Fig.1 shows the results of a calculation by Laget [12] for our proposed kinematics. The upper graph shows the predicted asymmetry in perpendicular kinematics A'_x , i.e. the spin of the target is aligned perpendicular to the q -vector in the scattering plane. The lower graph shows the asymmetry in parallel kinematics A'_z , here is the target spin aligned along the q -vector. In both graphs is the $(e, e'p)$ asymmetry different from zero, even at zero missing momentum (4-5%), i.e. on top of the quasielastic peak (effect of the S' -state).

We believe that these kinematics are well chosen. The predicted asymmetries in perpendicular kinematics get larger as one moves away from the quasielastic peak (relative contribution of the D-state increases). The maximum asymmetry is about 22% at a missing momentum of about 300 MeV/c. Fig. 1 also shows that the effect of final state interactions (FSI) and meson exchange currents (MEC) is negligibly small. The asymmetry in parallel kinematics is expected to be similar at the quasielastic peak (about 6-7%) but decreases as one probes the wavefunction at higher missing momenta (up to p_m values of about 250 MeV/c). Here the asymmetry indicates a larger sensitivity to MEC.

III. Rate Estimates

We plan to perform the experiment in Hall A using both HRS spectrometers. We estimated the expected event rates with a Monte Carlo code which is a modified version of the EGN code developed by van den Brand [15]. We used the most recent values for the Hall A HRC acceptances, i.e. a solid angle of 5 msr, an accepted target length of 8 cm, an a momentum acceptance $\Delta p/p$ is 9%. Since we plan to perform our experiment a Q^2 value of $1 \text{ GeV}^2/c^2$, the electron scattering angle will be 15.5° . Therefore, we will effectively accept a target length of 30 cm ($= 8 \text{ cm}/\sin(\vartheta_e)$). We assume a ^3He density of $2.5 \cdot 10^{20} \text{ atoms/cm}^3$ (see below for detailed target description) and a beam current of $15 \mu\text{A}$. The corresponding luminosity is $8.8 \cdot 10^{35} / \text{cm}^2/\text{s}$. (Note: we will use the same or a very similar target as in the already approved experiments E-94-010, E-94-021, and E-95-001.)

Table 1 summarizes some of our experimental parameters.

TABLE 1 *Experimental parameters for a Q^2 value of $1 \text{ GeV}^2/c^2$ at an incident beam energy of 4 GeV . The effective target length was taken to be $8 \text{ cm}/\sin(\vartheta_e)$.*

Q^2 [GeV^2/c^2]	ϑ_e [$^\circ$]	ϑ_q [$^\circ$]	E' [GeV]	eff. tgt. length [cm]	tgt. density [cm^{-2}]
1.0	15.5	54.3	3.463	30.0	$7.4 \cdot 10^{21}$

All cross-sections were calculated in PWIA with de Forest's CC1 off-shell description [?] and the ^3He 2-body breakup momentum distribution was taken from a fit to the data of Jans *et al.* [18]. In order to estimate the ^3He 3-body breakup rates we used the spectral function as calculated by Schulze and Sauer [17]. We used a pointlike target in our calculation.

Since we are going to use the technique of collisional spin-exchange with optically pumped Rb, we have to take into account that our target will also contain small amounts of nitrogen and rubidium. We plan to use a target with a ^3He volume density of $2.5 \cdot 10^{20} \text{ atoms/cm}^3$. Since we are going to use technique of collisional spin-exchange with optically pumped Rb, there will be small amounts of The Rb density will be of the order $6 \cdot 10^{14} \text{ atoms/cm}^3$ (^{85}Rb (72.165% of the natural Rb abundance) and ^{87}Rb (27.835% natural abundance)). The partial nitrogen (^{14}N) pressure will be about 100 torr (or $1.4 \cdot 10^{19} \text{ N/cm}^3$) at room temperature. In principle this will amount to a dilution factor due to $(e, e'p)$ reaction from the rubidium and nitrogen (note that we will collimate out the end windows of our target cell, so there will be no background contribution from the glass). However, since the focus of the experiment

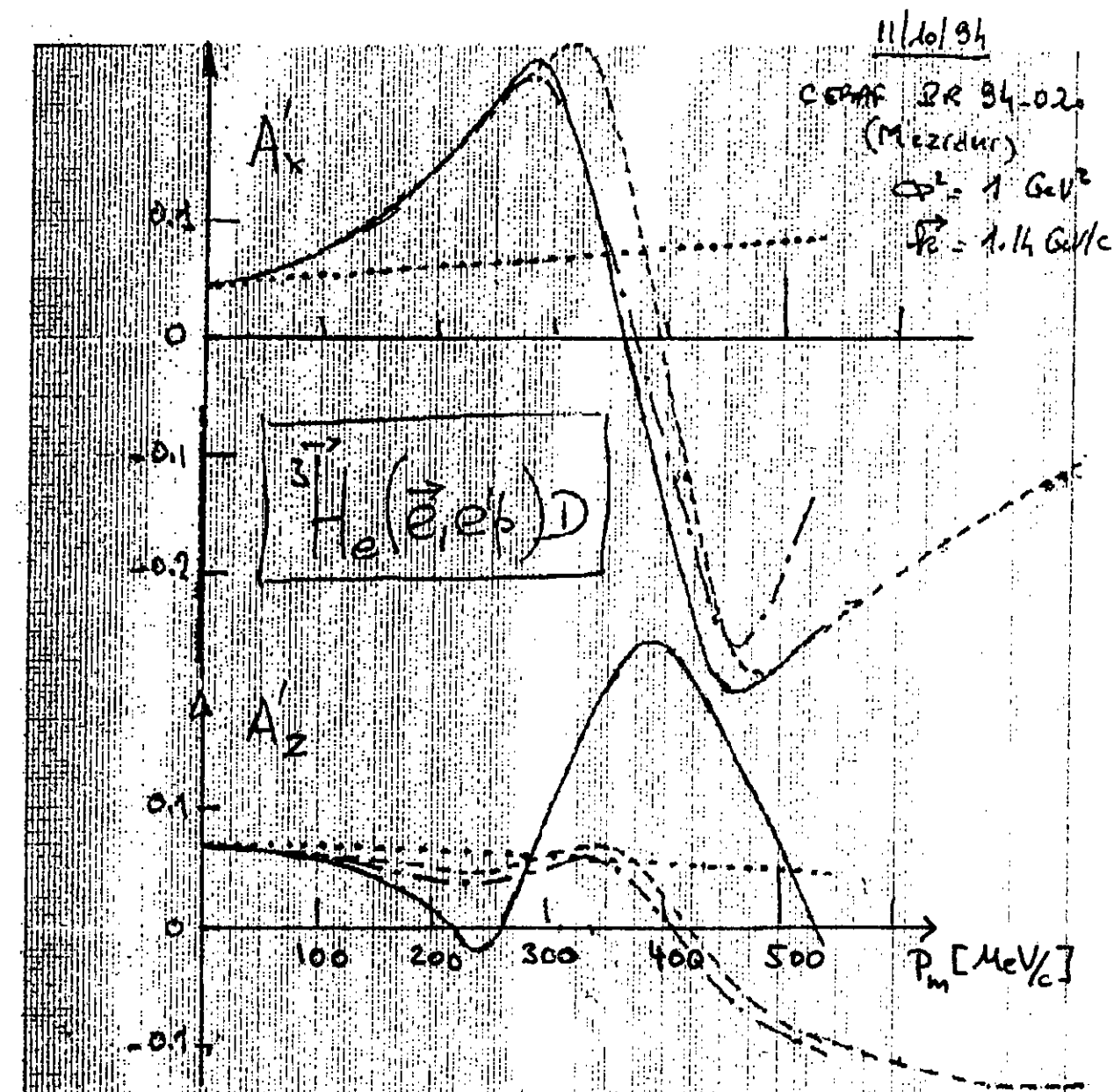


Figure 1: Expected asymmetries for the ${}^3\text{He}(\vec{e}, e'p)d$ reaction at a 4-momentum transfer of $1 \text{ GeV}^2/c^2$. The upper curve displays the asymmetry where target spin and photon momentum vector are aligned perpendicular to each other (A'_1). In the lower curve both vectors are aligned parallel (A'_2). The dotted curve is the effect from the S' -state, the dashed curve describes the effect of the S' and D -state. The dash-dotted line includes FSI and the solid line is the full calculation (with MEC).

is the two body break-up reaction and the resolution of the spectrometer is about 0.95 MeV (one σ) in our kinematics, we will be able to measure the 5.5 MeV two body break-up quite precisely. Therefore we should not see directly knocked out protons from N or Rb, since the separation energy for the 1p shell of nitrogen is about 17 MeV [19] and a simple Skyrme Hartree-Fock calculation [20] gives about 10 MeV separation energy for the 2p and 1f shell of rubidium. We certainly will perform careful background studies with “empty” (no ^3He in the target) target runs to enable reliable determination of the asymmetries in the 3 body breakup channel. The dominant part of the dilution factor for the 3-body breakup channel is generated by the nitrogen. We estimated the dilution factor by estimating the background rates using an independent particle shell model spectral function for $^{12}_6\text{C}$. This spectral function should be not too dissimilar from a $^{14}_7\text{N}$ spectral function. The dilution factors are listed in Table 2.

TABLE 2 *Expected uncertainties for A'_x and A'_z in the ${}^3\vec{\text{He}}(\vec{e}, e'p)d$ reaction. It is assumed that the beam polarization is 0.8 and the target polarization is 0.45.*

p_m [MeV/c]	dilution factor $7.7 < E_m < 20$ MeV	dilution factor $20 < E_m < 40$ MeV
$0 < p_m < 50$	0.99	0.88
$50 < p_m < 100$	0.97	0.74
$100 < p_m < 150$	0.94	0.72
$150 < p_m < 200$	0.94	0.85
$200 < p_m < 250$	0.99	0.99

The polarizations should be about 45 % for the target and 80 % for the beam. Here we assumed that a strained GaAs crystal can be used to get high beam polarization. Since these crystals have low quantum efficiencies (SLAC achieved 0.1-0.3 % with polarizations up to 80 %), we assumed a low beam current of 15 μA . The count rates and expected uncertainties for the two different asymmetries in the ${}^3\vec{\text{He}}(\vec{e}, e'p)d$ reaction are listed in detail in Table 3. All the errors are statistical only.

TABLE 3 *Expected uncertainties for A'_x and A'_z in the ${}^3\vec{\text{He}}(\vec{e}, e'p)d$ reaction. It is assumed that the beam polarization is 0.8 and the target polarization is 0.45.*

p_m [MeV/c]	N(10 days) $\vec{s} \perp \vec{q} (\rightarrow A'_x)$	ΔA	N(2 days) $\vec{s} \parallel \vec{q} (\rightarrow A'_z)$	ΔA
$0 < p_m < 50$	$3.66 \cdot 10^6$	$\pm 1.45 \cdot 10^{-3}$	$7.31 \cdot 10^5$	$\pm 3.25 \cdot 10^{-3}$
$50 < p_m < 100$	$3.84 \cdot 10^6$	$\pm 1.42 \cdot 10^{-3}$	$7.68 \cdot 10^5$	$\pm 3.17 \cdot 10^{-3}$
$100 < p_m < 150$	$1.18 \cdot 10^6$	$\pm 2.55 \cdot 10^{-3}$	$2.37 \cdot 10^5$	$\pm 5.71 \cdot 10^{-3}$
$150 < p_m < 200$	$1.64 \cdot 10^5$	$\pm 6.86 \cdot 10^{-3}$	$3.28 \cdot 10^4$	$\pm 1.53 \cdot 10^{-2}$
$200 < p_m < 250$	$2.73 \cdot 10^3$	$\pm 5.32 \cdot 10^{-2}$	$5.46 \cdot 10^2$	$\pm 1.19 \cdot 10^{-1}$

Simultaneously we will collect data for the 3-body breakup reaction.

Here we binned the data in 20 MeV bins for the missing energy and 50 MeV/c bins for the missing momentum. The rates above $p_m > 250$ MeV/c will be too small to extract any useful information. The expected rates are listed in Table 4 and Table 5.

TABLE 4 Expected uncertainties for A'_x and A'_z in the ${}^3\text{He}(\bar{e}, e'p)pn$ reaction. It is assumed that the beam polarization is 0.8 and the target polarization is 0.45. This table covers the missing energy range $7.7 \text{ MeV} < E_m < 20 \text{ MeV}$.

p_m [MeV/c]	N(10 days) $\vec{s} \perp \vec{q}(\rightarrow A'_x)$	ΔA	N(2 days) $\vec{s} \parallel \vec{q}(\rightarrow A'_z)$	ΔA
$0 < p_m < 50$	$1.17 \cdot 10^6$	$\pm 2.59 \cdot 10^{-3}$	$2.34 \cdot 10^5$	$\pm 5.79 \cdot 10^{-3}$
$50 < p_m < 100$	$1.33 \cdot 10^6$	$\pm 2.48 \cdot 10^{-3}$	$2.67 \cdot 10^5$	$\pm 5.54 \cdot 10^{-3}$
$100 < p_m < 150$	$3.37 \cdot 10^5$	$\pm 5.09 \cdot 10^{-3}$	$6.74 \cdot 10^4$	$\pm 1.14 \cdot 10^{-2}$
$150 < p_m < 200$	$3.11 \cdot 10^4$	$\pm 1.68 \cdot 10^{-2}$	$6.22 \cdot 10^3$	$\pm 3.75 \cdot 10^{-2}$
$200 < p_m < 250$	$4.57 \cdot 10^2$	$\pm 1.31 \cdot 10^{-1}$	$9.14 \cdot 10^1$	$\pm 3.23 \cdot 10^{-1}$

TABLE 5 $20 \text{ MeV} < E_m < 40 \text{ MeV}$. Rest same as Table 4.

p_m [MeV/c]	N(10 days) $\vec{s} \perp \vec{q}(\rightarrow A'_x)$	ΔA	N(2 days) $\vec{s} \parallel \vec{q}(\rightarrow A'_z)$	ΔA
$0 < p_m < 50$	$2.85 \cdot 10^4$	$\pm 1.87 \cdot 10^{-2}$	$5.70 \cdot 10^3$	$\pm 4.18 \cdot 10^{-2}$
$50 < p_m < 100$	$4.92 \cdot 10^4$	$\pm 1.69 \cdot 10^{-2}$	$9.85 \cdot 10^3$	$\pm 3.78 \cdot 10^{-2}$
$100 < p_m < 150$	$2.42 \cdot 10^4$	$\pm 2.48 \cdot 10^{-2}$	$4.84 \cdot 10^3$	$\pm 5.55 \cdot 10^{-2}$
$150 < p_m < 200$	$4.92 \cdot 10^3$	$\pm 4.66 \cdot 10^{-2}$	$9.85 \cdot 10^2$	$\pm 1.04 \cdot 10^{-1}$

Fig. 2 shows the size of the estimated errors for the ${}^3\text{He}(\vec{e}, e'p)d$ reaction.

The systematic errors will be dominated by the beam - and target polarizations. We will measure the beam polarization with the Moeller polarimeter which will be operational in Hall A and plan to get a relative uncertainty of 5 % or better. The target polarization will be monitored and measured using the NMR technique of adiabatic fast passage (see specific section on the target) . We assume an uncertainty in the target polarization of 5%. So the total systematic error is about 7 %.

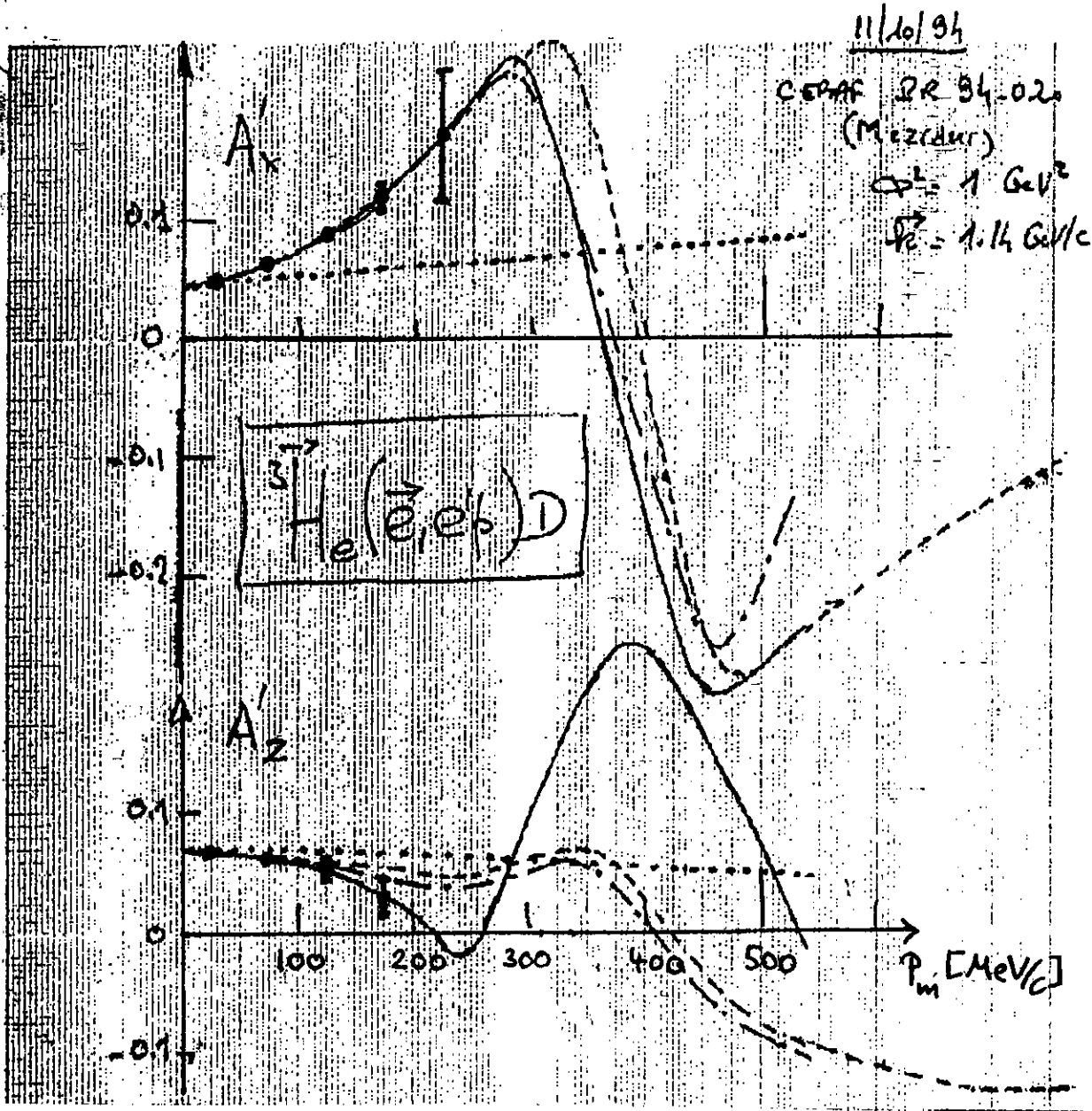


Figure 2: Expected asymmetries and statistical errors for the ${}^3\text{He}(\vec{e}, e'p)d$ reaction at a 4-momentum transfer of $1 \text{ GeV}^2/c^2$. The upper curve displays the asymmetry where target spin and photon momentum vector are aligned perpendicular to each other (A_1). In the lower curve both vectors are aligned parallel (A_2). The dotted curve is the effect from the S' -state, the dashed curve describes the effect of the S' and D -state. The dash-dotted line includes FSI and the solid line is the full calculation (with MEC).

IV. The Polarized ^3He Target

The polarized target will be based on the principle of spin exchange between optically pumped alkali-metal vapor and noble-gas nuclei [21, 22, 23]). The design will be similar in many ways to that used in E-142, an experiment at SLAC to measure the spin dependent structure function of the neutron [24]. A central feature of the target will be sealed glass target cells, which will contain a ^3He pressure of about 10 atmospheres. As indicated in Fig. 3, the cells will have two chambers, an upper chamber in which the spin exchange takes place, and a lower chamber, through which the electron beam will pass. In order to maintain the appropriate number density of alkali-metal (which will probably be Rb) the upper chamber will be kept at a temperature of 170–200°C using an oven constructed of the high temperature plastic Torlon. With a density of 2.5×10^{20} atoms/cm³, and a lower cell length of 40 cm, the target thickness will be 1.0×10^{22} atoms/cm².

We describe below in greater detail some features of the target.

1 Operating Principles

The time evolution of the ^3He polarization can be calculated from a simple analysis of spin-exchange and ^3He nuclear relaxation rates [25]. Assuming the ^3He polarization $P_{^3\text{He}} = 0$ at $t = 0$,

$$P_{^3\text{He}}(t) = \langle P_{\text{Rb}} \rangle \left(\frac{\gamma_{\text{SE}}}{\gamma_{\text{SE}} + \Gamma_{\text{R}}} \right) \left(1 - e^{-(\gamma_{\text{SE}} + \Gamma_{\text{R}})t} \right), \quad (2)$$

where γ_{SE} is the spin-exchange rate per ^3He atom between the Rb and ^3He , Γ_{R} is the relaxation rate of the ^3He nuclear polarization through all channels other than spin exchange with Rb, and $\langle P_{\text{Rb}} \rangle$ is the average polarization of a Rb atom. Likewise, if the optical pumping is turned off at $t = 0$ with $P_{^3\text{He}} = P_0$, the ^3He nuclear polarization will decay according to

$$P_{^3\text{He}}(t) = P_0 e^{-(\gamma_{\text{SE}} + \Gamma_{\text{R}})t}. \quad (3)$$

The spin exchange rate γ_{SE} is defined by

$$\gamma_{\text{SE}} \equiv \langle \sigma_{\text{SE}} v \rangle [\text{Rb}]_{\text{A}} \quad (4)$$

where, $\langle \sigma_{\text{SE}} v \rangle = 1.2 \times 10^{-19}$ cm³/sec is the velocity-averaged spin-exchange cross section for Rb– ^3He collisions([25, 26, 27]) and $[\text{Rb}]_{\text{A}}$ is the average Rb number density seen by a ^3He atom. Our target will be designed to operate with $1/\gamma_{\text{SE}} = 8$ hours.

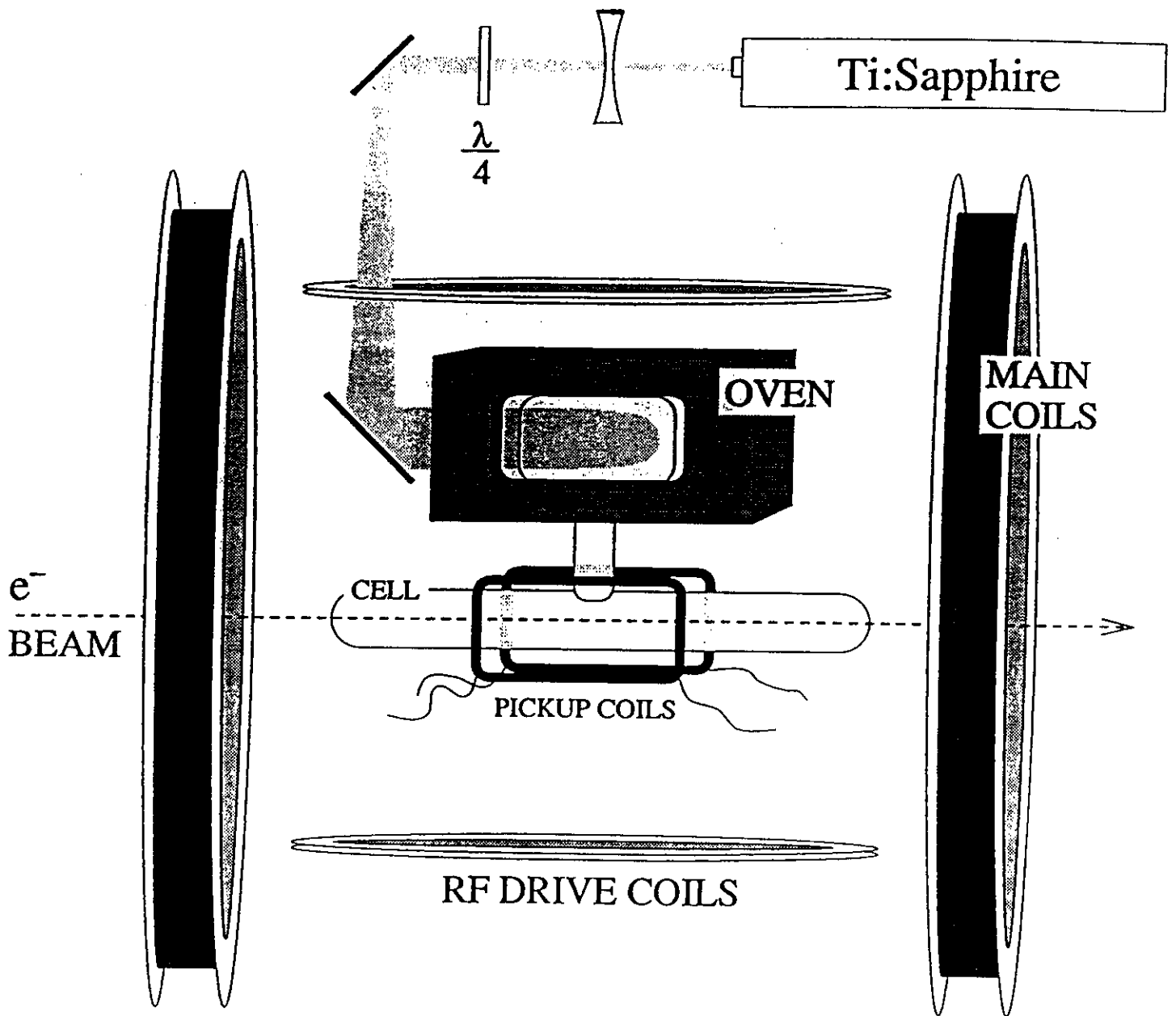


Figure 3

From Eq. (2) it is clear that there are two things we can do to get the best possible ^3He polarization — maximize γ_{SE} and minimize Γ_{R} . But from Eq. (7) it is also clear that maximizing γ_{SE} means increasing the alkali-metal number density, which in turn means more laser power. The number of photons needed per second must compensate for the spin relaxation of Rb spins. In order to achieve $1/\gamma_{\text{SE}} = 8$ hours, we will require about 24 Watts of usable laser light at a wavelength of 795 nm. We will say more about the source of laser light below.

The rate at which polarization is lost, which is characterized by Γ_{R} , will have four principle contributions. An average electron beam current of about 15 μA will result in a depolarization rate of $\Gamma_{\text{beam}} = 1/30$ hours [28]. Judging from experience at SLAC, we can produce target cells with an intrinsic rate of $\Gamma_{\text{cell}} = 1/50$ hours. This has two contributions, relaxation that occurs during collisions of ^3He atoms due to dipole-dipole interactions [29], and relaxation that is presumably due largely to the interaction of the ^3He atoms with the walls. Finally, relaxation due to magnetic field inhomogeneities can probably be held to about $\Gamma_{\nabla B} = 1/100$ hours [30]. Collectively, under operating conditions, we would thus expect

$$\Gamma_{\text{R}} = \Gamma_{\text{beam}} + \Gamma_{\text{cell}} + \Gamma_{\nabla B} = 1/30 \text{ hours} + 1/50 \text{ hours} + 1/100 \text{ hours} = 1/16 \text{ hours} . \quad (5)$$

Thus, according to Eq. 5, the target polarization cannot be expected to exceed

$$P_{\text{max}} = \frac{\gamma_{\text{SE}}}{\gamma_{\text{SE}} + \Gamma} = 0.66 . \quad (6)$$

Realistically, we will not achieve a Rb polarization of 100% in the pumping chamber, which will reduce the polarization to about 45–50%.

2 Target Cells

The construction and filling of the target cells must be accomplished with great care if $1/\Gamma_{\text{cell}}$ is to be in excess of 50 hours. We plan to use the “Princeton Prescription” which was developed for use in SLAC E-142. This resulted, among the cells that were tested, in lifetimes that were always better than 30 hours, and in about 60% of the cells, better than 50 hours. The following precautions will be taken:

- 1. Cells will be constructed from aluminosilicate glass.
- 2. All tubing will be “resized.” This is a process in which the diameter of the tubing is enlarged by roughly a factor of two in order to insure a smooth pristine glass surface that is free of chemical impurities.
- 3. Cells will be subjected to a long (4–7 day) bake-out at high ($> 400^\circ\text{C}$) temperature on a high vacuum system before filling.

- 4. Rb will be doubly distilled in such a manner as to avoid introducing any contaminants to the system.
- 5. The ^3He will be purified either by getters or a liquid ^4He trap during filling.

The cells will be filled to a high density of ^3He by maintaining the cell at a temperature of about 20 K during the filling process. This is necessary so that the *pressure* in the cell is below one atmosphere when the glass tube through which the cell is filled is sealed.

The length of the cell has been chosen to be 40 cm so that the end windows will not be within the acceptance of the Hall A spectrometers. The end windows themselves will be about $100\ \mu$ thick. Thinner windows could in principle be used, but this does not appear to be necessary.

3 The Optics System

As mentioned above, approximately 20–24 Watts of “usable” light at 795 nm will be required. By “usable,” we essentially mean light that can be readily absorbed by the Rb. It should be noted that the absorption line of the Rb will have a full width of several hundred GHz at the high pressures of ^3He at which we will operate. Furthermore, since we will operate with very high Rb number densities that are optically quite thick, quite a bit of light that is not within the absorption linewidth is still absorbed.

It is our plan to take advantage of new emerging diode laser technology to economically pump the target. Systems are now commercially available in which a single chip produces about 20 watts of light, about half of which is probably usable. Between 2–4 such systems, at a cost of about \$25,000 each, should do the job. There is also a group at Lawrence Livermore Laboratory that has offered to build us a single chip that can produce 150 watts. While some studies of the use of diode lasers for spin-exchange optical pumping do exist in the literature [31], actual demonstrations of high polarizations in cells suitable for targets are much more recent [32]. It is our opinion that diode lasers will probably work, but we will perform several tests before freezing this decision.

At SLAC, five titanium-sapphire/argon ion laser systems were used to drive the E-142 polarized ^3He target. This option will definitely work, but is much more expensive.

4 Polarimetry

Polarimetry will be accomplished by two means. During the experiment, polarization will be monitored using the NMR technique of adiabatic fast passage (AFP) [33].

The signals will be calibrated by comparing the ^3He NMR signals with those of water. The calibration will be independently verified by studying the frequency shifts that the polarized ^3He nuclei cause on the electron paramagnetic resonance (EPR) lines of Rb atoms [28]. This second techniques will be performed in separate target studies, not during the experiment. It will serve solely as a check of our calibration. We plan to determine the polarization of the target to within 5% of itself.

5 Apparatus Overview

The target will be in air or, perhaps, in a helium bag. This greatly simplifies the design. The main components of the target are shown in Fig. 3.

The “main coils” shown are large Helmholtz coils that will be used to apply a static magnetic field of about 20 Gauss. In addition to establishing the quantization axis for the target, the main coils are important for suppressing relaxation due to magnetic field inhomogeneities, which go like $1/B^2$. At 20 G, inhomogeneities can be as large as about 30 mG/cm while keeping $\Gamma_{\nabla B} < 1/100\text{hours}$. By increasing the applied field to about 40 G, and relaxing our requirements on $\Gamma_{\nabla B}$ by about factor of two, inhomogeneities as large as 0.25 G/cm can be tolerated. We are still finalizing our final choice of static field.

The NMR components in the target include a set of RF drive coils, and a separate set of pick-up coils. Not shown in the figure are the NMR electronics, which include an RF power amplifier, a lock-in amplifier, some bridge circuitry, and the capability to sweep the static magnetic field.

The oven shown in Fig. 3 is constructed of Torlon, a high temperature plastic. The oven is heated with forced hot air.

The optics system will either include five Ti:sapphire lasers (only one is shown) or 2–4 laser diode systems. Either way, there will also be several lenses and a quarter wave plate to provide circular polarization.

V. Contribution of the Collaboration and Beam Time Request

- Construction and installation of the polarized ^3He target. This includes Helmholtz coils for the target guiding field and target polarimeter.

We request from Jefferson Lab:

- Polarized beam of $15\mu\text{A}$ and a beam polarization of 80% at a beam energy of 4 GeV.
- Support for target installation.
- Beam pipe instrumentation, i.e. beam position and beam current monitors.
- Working polarimeter to measure the beam polarization.

Further we request a total running time of 360 hrs to perform the complete experiment. We will need 300 hrs for the production run, about 24 hrs for beam polarization measurements (about 2 hours per day), 10% of the data taking for background studies, i.e. 30 hrs. We would like to point out that our collaboration has already 3

approved experiments using a polarized ^3He target in Hall A and is strongly involved in the development of the infrastructure for the installation of the target in Hall A (e.g. support structure for the target, field gradient measurements, high pressure in-beam cell tests) We also certainly will get lots of target experience during the first already approved experiments (E-94-010, E-94-021, and E-95-001) and can take advantage of all the infrastructure which will be developed for these experiments. This will amount in fast installation time and will therefore minimize the downtime of the accelerator.

References

- [1] HERMES Collaboration, Proposal to measure the spin-dependent structure functions of the neutron and the proton at HERA.
- [2] K. Lee *et al.*, *Phys. Rev. Lett.* **70**, 738 (1993).
- [3] H. Gao *et al.*, *Phys. Rev. C* **50**, R546 (1994).
- [4] C. Jones *et al.*, *Phys. Rev. C* **47**, 110 (1993).
- [5] M. Meyerhoff *et al.*, *Phys. Lett. B* **327**, 201 (1994).
- [6] E142 Collaboration, P.L Anthony *et al.*, *Phys. Rev. Lett.* **71**, 959 (1993); E154-Collaboration, Proposal to measure the spin-dependent structure function g_1^n of the neutron at SLAC.
- [7] E-94-010, spokespersons: G. Cates and Z.E. Meziani, "Measurement of the Neutron (^3He) Spin Structure Function at Low Q^2 ; a Connection between the Bjorken and Drell-Hearn-Gerasimov Sum Rules"; E-94-021, spokespersons: W. Korsch and R. McKeown, "The Electric Form Factor of the Neutron Extracted from the $^3\vec{\text{He}}(\vec{e}, e'n)pp$ Reaction"; E-95-001, spokesperson: H. Gao, "Precise Measurement of the Inclusive Spin-dependent Quasi-elastic Transverse Asymmetry A_{TV} from $^3\vec{\text{He}}(\vec{e}, e')$ at low Q^2 ".
- [8] J. Golak, S. Ishikawa, and W. Glöckle, private communication.
- [9] J. Golak, S. Ishikawa, and W. Glöckle, private communication.
- [10] J.L. Friar *et al.*, *Phys. Rev. C* **42**, 2310 (1990).
- [11] M.A Miller *et al.*, *Phys. Rev. Lett.* **74**, 502 (1995).
- [12] J.M. Laget, private communication.
- [13] J.M. Laget, *Phys. Lett. B* **276**, 398 (1992).
- [14] T.W. Donnelly, private communication.
- [15] J.v.d. Brand, private communication.
- [16] T. de Forest, *Nucl. Phys. A* **392**, 232 (1983).
- [17] R.W. Schulze and P.U. Sauer, *Phys. Rev. C* **48**, 38 (1993).
- [18] E. Jans *et al.*, *Nucl. Phys. A* **475**, 687 (1987).
- [19] S. Frullani and J. Mougey, *Adv. Nucl. Phys.* **14**, 1 (1984).

- [20] P.-G. Reinhard, Computational Nuclear Physics 1 (Springer), K. Langanke, J.A. Mahrun, S.E. Koonin (Edts).
- [21] M.A. Bouchiat, T.R. Carver and C.M. Varnum, *Phys. Rev. Lett.* **5**, 373 (1960).
- [22] N.D. Bhaskar, W. Happer, and T. McClelland, *Phys. Rev. Lett.* **49**, 25 (1982).
- [23] W. Happer, E. Miron, S. Schaefer, D. Schreiber, W.A. van Wijngaarden, and X. Zeng, *Phys. Rev. A* **29**, 3092 (1984).
- [24] E142 Collaboration, P.L Anthony *et al.*, *Phys. Rev. Lett.* **71**, 959 (1993).
- [25] T.E. Chupp, M.E. Wagshul, K.P. Coulter, A.B. McDonald, and W. Happer, *Phys. Rev. C* **36**, 2244 (1987).
- [26] K.P. Coulter, A.B. McDonald, W. Happer, T. E. Chupp, and M.E. Wagshul, *Nucl. Instrum. Methods A* **270**, 90 (1988).
- [27] N.R. Newbury, A.S. Barton, P. Bogorad, G. D. Cates, M. Gatzke, H. Mabuchi, and B. Saam, *Phys. Rev. A* **48**, 558 (1993).
- [28] K.P. Coulter, A.B. McDonald, G.D. Cates, W. Happer, T.E. Chupp, *Nucl. Instrum. Methods A* **276**, 29 (1989).
- [29] N. R. Newbury, A. S. Barton, G. D. Cates, W. Happer, and H. Middleton, *Phys. Rev. A* **48**, 4411 (1993).
- [30] G.D. Cates, S.R. Schaefer and W. Happer, *Phys. Rev. A* **37**, 2877 (1988); G.D. Cates, D.J. White, Ting-Ray Chien, S.R. Schaefer and W. Happer, *Phys. Rev. A* **38**, 5092 (1988).
- [31] M. E. Wagshul and T. E. Chupp, *Phys. Rev. A* **40**, 4447 (1989).
- [32] B. Cummings, private communication.
- [33] A. Abragam, Principles of Nuclear Magnetism (Oxford University Press, New York, 1961).